Lohtander, Tia; Grande, Rafael; Österberg, Monika; Laaksonen, Päivi; Arola, Suvi

Bioactive Films from Willow Bark Extract and Nanocellulose Double Network Hydrogels

Published in:
Frontiers in Chemical Engineering

DOI:
10.3389/fceng.2021.708170

Published: 12/08/2021

Document Version
Publisher's PDF, also known as Version of record

frontiers in Chemical Engineering

ORIGINAL RESEARCH
published: 12 August 2021
doi: 10.3389/fceng.2021.708170

Bioactive Films from Willow Bark Extract and Nanocellulose Double Network Hydrogels

*Tia Lohtander[1,2], Rafael Grande[2], Monika Österberg[2], Päivi Laaksonen[3] and Suvi Arola[1]**

[1]*Biomass Processing and Products, VTT Technical Research Centre of Finland Ltd., Espoo, Finland,* [2]*Department of Bioproducts and Biosystems, School of Chemical Engineering, Aalto University, Espoo, Finland,* [3]*HAMK Tech. Häme University of Applied Sciences, Hämeenlinna, Finland*

In nature, the protection of sensitive components from external threats relies on the combination of physical barriers and bioactive secondary metabolites. Polyphenols and phenols are active molecules that protect organisms from physical and chemical threats such as UV irradiation and oxidative stress. The utilization of biopolymers and natural bioactive phenolic components as protective coating layers in packaging solutions would enable easier recyclability of materials and greener production process compared with the current plastic-based products. Herein, we produce a fully wood-based double network material with tunable bioactive and optical properties consisting of nanocellulose and willow bark extract. Willow bark extract, embedded in nanocellulose, was cross-linked into a polymeric nanoparticle network using either UV irradiation or enzymatic means. Based on rheological analysis, atomic force microscopy, antioxidant activity, and transmittance measurements, the cross-linking resulted in a double network gel with enhanced rheological properties that could be casted into optically active films with good antioxidant properties and tunable oxygen barrier properties. The purely biobased, sustainably produced, bioactive material described here broadens the utilization perspectives for wood-based biomass, especially wood-bark extractives. This material has potential in applications where biodegradability, UV shielding, and antioxidant properties of hydrogels or thin films are needed, for example in medical, pharmaceutical, food, and feed applications, but also as a functional barrier coating in packaging materials as the hydrogel properties are transferred to the casted and dried films.

Keywords: cellulose nanofibrils, wood-bark extracts, double network hydrogels, bioactive (poly)phenols, barrier properties, polyphenols, laccase

OPEN ACCESS

Edited by:
Tiina Nypelö,
Chalmers University of Technology, Sweden

Reviewed by:
Heather Trajano,
University of British Columbia, Canada
Hany Elazab,
British University in Egypt, Egypt

****Correspondence:***
Suvi Arola
suvi.arola@vtt.fi

Specialty section:
This article was submitted to Chemical Reaction Engineering, a section of the journal Frontiers in Chemical Engineering

Received: *11 May 2021*
Accepted: *30 June 2021*
Published: *12 August 2021*

Citation:
Lohtander T, Grande R, Österberg M, Laaksonen P and Arola S (2021) Bioactive Films from Willow Bark Extract and Nanocellulose Double Network Hydrogels. Front. Chem. Eng. 3:708170. doi: 10.3389/fceng.2021.708170

INTRODUCTION

Packaging and encapsulation of food, drugs, and other sensitive compounds needing protection against gaseous and microbial attacks and light are designed to ensure a long enough shelf-life and safe consumption of the contents. Many packages are composite products consisting of layers of synthetic polymers and other materials to ensure sufficient barrier properties and mechanical performance, and are challenging to recycle or dispose without producing waste (Kaiser et al., 2018). In nature, tree barks represent an excellent solution for the preservation of sensitive contents, as they provide the trees' effective protective layers that eventually decay among the other parts of the tree

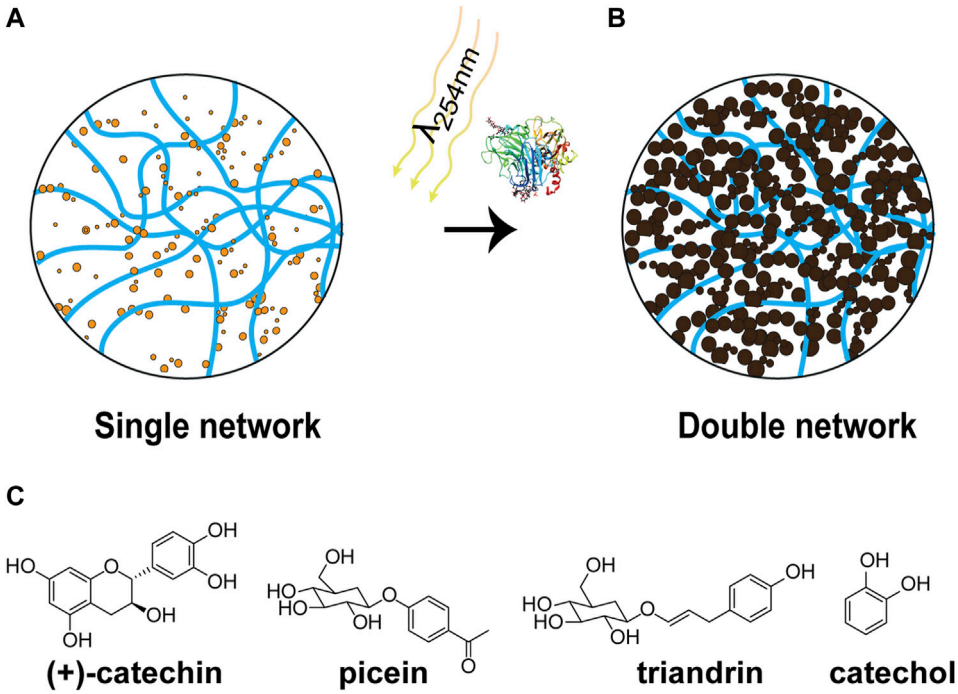

FIGURE 1 | Formation of double network gels from TEMPO-oxidized cellulose nanofibrils (TCNF) and willow bark extract (WBE). **(A)** Single network of TCNF mixed with WBE. **(B)** Second network of WBE is polymerized around the TCNF network forming a double network. The polymerization is done via UVC irradiation or enzymatic reaction. **(C)** WBE components and catechol.

and circulate fully in the ecosystem. The bark provides mechanical and chemical protection against external threats such as UV radiation and attacks from pathogens, giving the tree cells an opportunity for extended life span (Pásztory et al., 2016). In this work, we describe a biomimetic route to wood-derived materials applicable as bio-active barrier in packaging or encapsulation.

Double network (DN) hydrogels are a promising approach to enhance the performance of hydrogels (Gong, 2010). In general, DN hydrogels are formed by two entangled gel networks that are not linked to each other. The primary hydrogel is vastly cross-linked, tough, and strong and the second hydrogel network is less cross-linked, soft, and ductile (**Figures 1A,B**). Combined they have mechanically superior properties compared with their components alone (Chen et al., 2015). In this study, we create and characterize a double network of cellulose nanofibrils and cross-linked willow bark extract. Besides the densely packed and mechanically sturdy gel structure, this approach allows embedding the bioactive functionality of the willow bark constituents into the nanocellulose matrix.

Traditionally, plant extracts have been applied for instance as medicinal and nutritional products (Quideau et al., 2011), in leather tanning (Covington, 1997), and textile coloration (Bechtold et al., 2003), but due to the emergence of synthetic production of chemical substances and industrialization, the use of natural extracts has become limited to only certain segments, such as cosmetics and health care. Natural plant extracts include a vast range of different bioactive compounds, such as alkaloids, steroids, tannins, glycosides, phenols, and flavonoids, often enriched at different parts of the plants (Altemimi et al., 2017). Polyphenols exhibit bioactivity, such as antioxidant, antimicrobial, and anticarcinogenic properties, and in addition they have an ability to precipitate proteins and act as metal chelators (Quideau et al., 2011; Li et al., 2014; Brglez Mojzer et al., 2016). Recently, due to the growing interest in more sustainable ways of creating functional and active materials the research around plant polyphenols has emerged. Natural polyphenol complexes have been introduced for instance in sustainable packaging (Missio et al., 2018), biomedical applications (Zhang et al., 2020), superhydrophobic materials (Wang et al., 2021), adhesives (Moubarik et al., 2009), preservatives in wood products (Tondi et al., 2013a), water purification (Sánchez-Martín et al., 2011), and as natural dyes (Lohtander et al., 2019). Polyphenols can be feasibly derived from existing, abundant side-streams of forest industry, such as tree barks, which are currently underutilized and often burned for energy production (Pietarinen et al., 2006; Feng et al., 2013; Ajao et al., 2021). The most commonly used methods for obtaining plant extracts are based on scalable solvent extraction with water or other polar solvents (Tsao and Deng, 2004).

Cellulose is a structural polymer found in abundance for example in plant-based biomass. Cellulose fibers can be disintegrated into different derivatives of cellulose nanofibrils (CNF) with various mechanical, chemical, and enzymatic top-down methods (Abe et al., 2007). In TEMPO-oxidized cellulose nanofibrils (TCNF), the C6 primary hydroxyls of the elemental

fibrils that are exposed to solvent are converted to sodium carboxylates, which result in individualized fibrils with unique properties, such as high aspect ratio, high surface charge, large surface area, and outstanding mechanical strength (Isogai et al., 2011). The large number of chemically reactive carboxylate groups on the fiber surface makes TCNF an interesting matrix for adsorption of hydroxyl group containing polyphenols. The adsorption of polyphenols to cellulose involves a combination of hydrogen bonds and hydrophobic interaction (Phan et al., 2015). The entangled individual nanocellulose fibrils form a 3D colloidal hydrogel network with high water content and an ability to swell (De France et al., 2017). Hydrogels from polymeric materials and CNF have been utilized in applications, such as artificial tissue scaffolds (Drury and Mooney, 2003; Bhattacharya et al., 2012; Yliperttula et al., 2013), drug delivery (Hoare and Kohane, 2008), and agriculture (Abd El-Rehim, 2006), to mention a few. However, often the single-component hydrogels have limited mechanical properties. CNF materials also show very good oxygen and oil barrier properties as films due to the vast hydrogen bonding network formed between fibrils when dried. The CNF forms nanostructured films, and this in turn also increases the barrier properties. The possibility of chemically modifying the CNF fibrils allows functional surface coatings and modified barriers properties with, for example, increased water vapor barrier properties (Hubbe et al., 2017; Wang et al., 2018).

As the interaction between polyphenols and cellulose is non-covalent in nature, the bioactive properties of cellulose functionalized with adsorbed polyphenols leach quite easily (Tondi et al., 2013b). To improve the stability, immobilization of different polyphenols to polymer matrices via covalent bonds has been performed with chemical approaches (Delgado-Sánchez et al., 2016; Hu et al., 2017). Here, we demonstrate that the durability of the bioactive properties of cellulose-based material can also be achieved with mild process conditions utilizing the characteristic reactions of polyphenols and physical entanglement. Phenolic compounds can undergo polymerization via enzymatic, chemical, and even auto-oxidation reactions (Tanaka et al., 2010). Also, light irradiation can alter the structures of phenolics as photoinduced excitation of hydroxyl groups and aromatic ring can lead to new isomers and oligomeric products (Yu et al., 2014; Shi et al., 2016). In the present work, we use these methods to create a double network (DN) gel by creating internal cross-links in the willow bark extract, which leads to interlocking with the nanocellulose fibril network (**Figures 1A,B**). Hot water extraction was employed for obtaining the willow bark extract whose main constituents are (+)-catechin, picein, and triandrin, along with some free monosugars (**Figure 1C**) (Dou et al., 2018). The oxidation and polymerization mechanisms of (+)-catechin have been thoroughly investigated and the reaction is known to occur through the catechol moiety on the B-ring of catechin (Torreggiani et al., 2008). Catechol is polymerized with the same reaction mechanisms and thus catechol was selected as a model compound for plant polyphenol in this study (Solano, 2014). The properties, formation mechanism, and bioactivity of films formed by casted DN gels were studied and it was shown that the properties could be tuned via mild process conditions using UV irradiation and enzymatic means.

MATERIALS AND METHODS

Materials

TEMPO-oxidized nanocellulose (TCNF) with a surface charge of 1 $mmolg^{-1}$ was prepared from bleached birch kraft pulp, as described earlier by Saito et al. (2007). Shortly, never dried bleached birch kraft pulp at 1 $g\,L^{-1}$ concentration was subjected to TEMPO catalyzed oxidization (0.3 weight ratio of TEMPO to pulp) for 4 h at room temperature. The product was purified from residual reaction chemicals by centrifugation and re-dispersing with deionized water. The centrifugation and washing step were repeated twice. The resulting TEMPO–CNF was then fluidized twice using 1,300 bar and 1900 bar pressure respectively with a fluidizer (Microfluidics M110EH). The carboxylic acid content of TEMPO–CNF (dry matter content 1.06% w/w) was determined by conductometric titration and was approximately 1 $mmolg^{-1}$. Willow bark extract (WBE) was obtained from barks of four-year-old hybrids (Karin, harvested from Finland, Kyyjärvi plantation) using hot water extraction (bark-to-water ratio 1:20) at 80°C for 30 min with stirring at 250 rpm according to the previously published method (Dou et al., 2018). The extract was filtered (retention size 12–15 μm) and centrifuged (4,500 g, 20 min, 21°C) to remove residual bark solids, and lyophilized into powder. The main components of extract were picein, (+)-catechin, triandrin, and monosugars (~29%, ~11%, ~25%, and 26.5%, respectively) according to an earlier study (Dou et al., 2018). A *Trametes hirsuta* laccase (*Th*L) with a catalytic activity of 6,500 nkat ml^{-1} and a protein concentration of 3.5 $g\,L^{-1}$ was homologically produced, and purified with a method described elsewhere (Rittstieg et al., 2002). Catechol (Cat, purity ≥99%), ABTS (2,2′-azino-bis(3-ethylbenzothiazoline-6-sulfonic acid)), D-sorbitol (≥98%), and tannic acid (ACS grade) were obtained from Sigma-Aldrich (Helsinki, Finland). The water used in all experiments was purified with a Millipore Synergy UV unit (MilliQ-water, 18.2 MΩcm).

Preparation of Gels and Films

The double network hydrogels of TCNF with WBE or catechol were made according to the procedure presented in **Scheme 1** and then cast to form the self-standing films. First, the WBE or catechol was mixed with TCNF network and polymerized *in situ* by using a *Trametes hirsuta* laccase (*Th*L) or UVC-light to yield a double network hydrogel, and second, a self-standing nanocomposite film with the bioactive properties was casted.

TCNF suspension of 0.4 wt% (4 $g\,L^{-1}$) and 0.8 wt% (8 $g\,L^{-1}$) aqueous solution of WBE or catechol was mixed properly with a magnetic stirrer. The pH of used WBE and catechol solutions were 5.4 and 4.4, respectively. The final concentration of TCNF was 0.2 wt% and that of WBE or catechol was 0.4 wt%. Double network (DN) hydrogels were prepared by polymerization of phenols either as a bulk reaction with laccase enzyme or as a surface irradiation with UV-light. The concentration of *Th*L in the enzymatically polymerized samples was 20 nkat ml^{-1} and the samples were incubated at 37.5°C for 4 h with constant shaking. UV-irradiated samples were exposed to UVC (254 nm) light

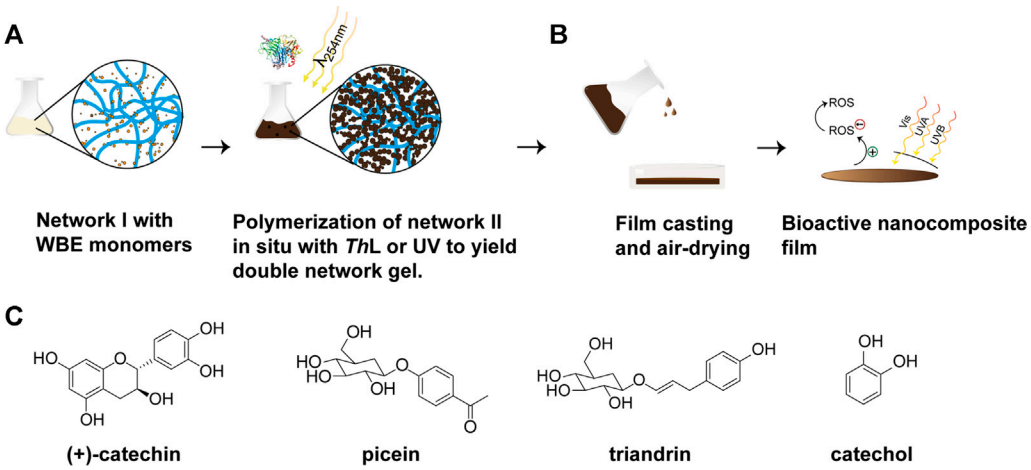

SCHEME 1 | The procedure of preparing double network hydrogels and bioactive nanocomposite films from TEMPO-oxidized cellulose nanofibrils (TCNF) and willow bark extract (WBE) or catechol. **(A)** Network I (TCNF) is mixed with network II monomers (WBE or catechol). Network II is formed from WBE or catechol by polymerization reaction with *Th*L laccase enzyme or UV-light. **(B)** Nanocomposite film is formed by casting and air-drying. Bioactivity tests are carried out for the nanocomposite films.

using UV cross-linker CL-508 (Uvitec, United Kingdom) and the applied exposure was 40 Jcm^{-2}. For film preparation, the DN gels were casted on polystyrene petri dishes (diameter 6 cm) and dried under ambient conditions for 3 days to ensure equilibration and full dryness. For the analysis of the films the dry matter content of materials was doubled but the ratio of TCNF to WBE/catechol was kept constant, i.e., 0.4 wt% TCNF and 0.8 wt% WBE or catechol. For oxygen transmission rate analysis, the films were plasticized with sorbitol (30 wt% of TCNF dry matter) to keep the self-standing films intact during the measurements. Sorbitol was mixed into the DN mixtures prior to film casting.

Chemical Analysis

The UVC-light and *Th*L enzymatically cross-linked polymeric materials of 0.4 wt% WBE or catechol were characterized using size-exclusion chromatography (SEC). Polymeric materials were dissolved into 0.1 M NaOH to a concentration of 2 g L^{-1} and filtered through a Millex 0.45 µm syringe filter (Millipore, United States). A high-performance liquid chromatography system (Agilent 1,100, Agilent Technologies, United States) was used in combination with a UV detector, and the applied flow rate was 0.7 mL min^{-1}, and injection volume 50 µL. Molar masses were determined based on the UV signal at 280 nm and columns used were Polymer Standards Service MCX 300 X 8 mm (three columns with pore sizes of 100 Å, 500 Å, and 1,000 Å). Calibration curve was accomplished with polystyrene sulfonate standards (1,000–64,000 g mol^{-1}) and syringol (M = 154 g mol^{-1}).

The changes in chemical structure of suspension-casted films were measured using attenuated total reflection Fourier-transform infrared (ATR FTIR) spectroscopy. FTIR spectra were obtained with a Thermo Scientific Nicolet iS50 FT-IR spectrometer coupled with an attenuated total reflection (ATR) diamond (Thermo Scientific, United States). The spectra were normalized relative to the band at 1,026 cm^{-1}.

Bioactive Properties

UV protective properties and antioxidant activity of suspension-casted films were measured with a UV-2550 spectrophotometer (Shimadzu, Japan). Antioxidant activity of suspension-casted films and pure compounds were determined according to ABTS assay reported elsewhere (Re et al., 1999) with small modifications. Briefly, the stock solution of ABTS radical cation was diluted with water until absorbance reading 0.7 at 734 nm. The samples, powder (2 mg) or circular films (d = 6 mm), were mixed with 2 ml of diluted radical solution. Tannic acid (TA) was used as antioxidant reference and the calibration curve was prepared from five different concentrations (0.1–2 µgmL^{-1}). The absorbance was recorded after mixing samples with a rotator for 30 min and all measurements were carried out in triplicates.

The ABTS radical scavenging activity was calculated using equation

$$\textit{Radical scavenging}\,(\%) = \left(\frac{1 - A_s}{A_c}\right)x100 \qquad (1)$$

where A_s is the absorbance of the sample after the reaction and A_c is the absorbance of the ABTS radical cation solution. Results were reported also as tannic acid (TA) equivalents, which were calculated with a calibration curve (**Supplementary Figure 6A**).

Physical Properties

The adsorption of WBE onto TCNF thin film was investigated using quartz crystal microbalance with dissipation monitoring (QCM-D). TCNF thin films were spin-coated onto gold quartz crystals (Q-Sense, Biolin Scientific, Sweden) using polyethyleneimine (PEI) as an anchoring layer. First, drops of PEI solution were deposited on the crystals and the polymer was allowed to adsorb for 10 min, and then, the crystals were thoroughly rinsed with deionized water. The 1.2 wt% suspension of TCNF was centrifuged (8,000 × g, 30 min) to

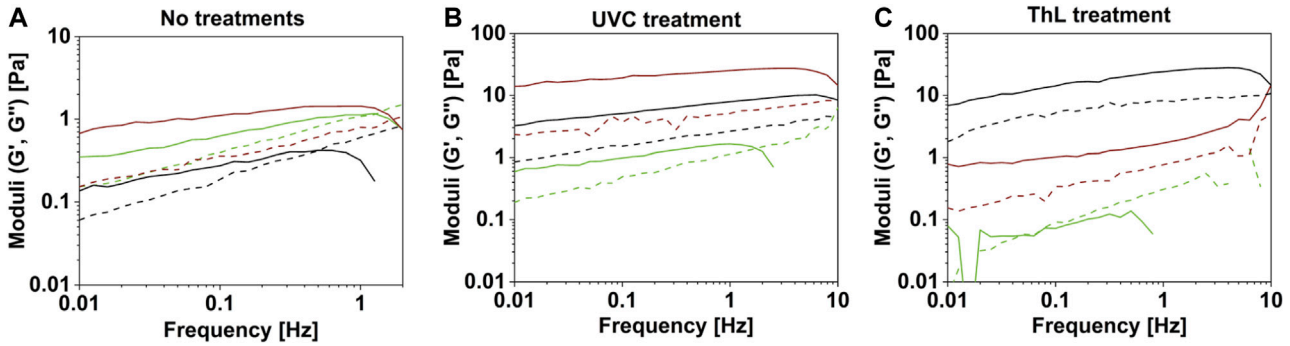

FIGURE 2 | Small deformation frequency sweeps of double network gels of TEMPO-oxidized cellulose nanofibril (TCNF) with willow bark extract (WBE) or catechol and TCNF controls. **(A)** Untreated TCNF (green lines), TCNF with WBE (brown lines), and TCNF with catechol (black lines), **(B)** UVC cross-linked TCNF (green lines), TCNF with WBE (brown lines), and TCNF with catechol (black lines), and **(C)** *Th*L enzyme cross-linked of TCNF (green lines), TCNF with WBE (brown lines), and TCNF with catechol (black lines). Solid lines in figures represent the elastic modulus (G′) and dashed lines represent the viscous modulus (G″).

obtain finest fibrils containing supernatant (0.15 wt%), which was then spin-coated (4,000 rpm, 1 min) onto crystals. Lastly, the substrates were heated at 165°C for 5 min followed by cleaning under flowing nitrogen. The increase in the sensed mass and viscoelastic properties of TEMPO-oxidized cellulose nanofibril thin film due to adsorption of willow bark extract (WBE) was monitored using a Q-Sense E4 instrument (Q-sense, Sweden) at room temperature. A constant flow rate of 100 μL min^{-1} was applied in all measurements. First, deionized water was injected until a stable baseline was obtained. Then WBE solution (0.1 g L^{-1}) was injected until the monitored resonance frequency of the quartz crystal (5 MHz) becomes stable. Finally, the chambers were rinsed with deionized water until the monitored resonance was stable. WBE adsorption was followed as changes in the resonance frequency (3^{rd} overtone) of the QCM-D sensor.

The surface morphology was characterized from spin-coated thin films by using atomic force microscopy (AFM). The AFM imaging was performed with a Nano-TA instrument (Anasys Instruments, United States) using tapping mode in air with mounted standard silicon tapping mode probes with Al reflex coating (Applied Nanostructures Inc., CA, United States) and only flattening was used in image processing. The size of images was 5 × 5 $μm^2$ and images were taken from two different locations of samples. The size of polymeric particles was estimated from the cross-section profiles of height images. The damping ratio in imaging was between 0.75 and 0.85.

Oxygen transmission rate (OTR) of suspension-casted films was measured according ASTM standard F1927 using gas permeation tester (Mocon Ox-Tran Model 2/21, Modern Controls Inc., United States). The sample film was masked between metal foils and measured under controlled conditions (RH 50%, 23°C) from 5 cm^2 area. Duplicate samples were analyzed simultaneously. Thickness of films was measured with a micrometer (Lorentzen and Wettre, Sweden) from three places and given as a mean value. The stability of films' color was qualitatively tested by immersing film pieces to water for 30 min and the color leaching was recorded with photographs before and after immersion.

Tensile strength testing was carried out with a DDS-3 microtensile tester (Kammrath & Weiss, Germany) using 100 N load cell, 10 mm gauge length, and 0.5 mm min^{-1} elongation rate. The casted films with known thickness were cut into 2.25 mm × 10 mm specimens with razor blade jig and each specimen was glued from both ends to small paper pads. Samples were equilibrated at 50% relative humidity and 21°C at least for 12 h prior to measurements. The mean tensile strength and toughness were determined from four measurements.

Rheological measurements were performed with a smooth 40 mm parallel plate geometry using Discovery hybrid rheometer-2 (TA Instruments, United States). The concentration of TCNF was 0.2 wt% and that of WBE/catechol was 0.4 wt%. Frequency sweeps were carried out at 22°C using frequencies 0.01–10 Hz with constant stress determined individually to each sample type with oscillatory stress sweeps to ensure that the measurements were performed at the linear visco-elastic region. Stress sweeps (0.001–1 Pa) were performed using a constant frequency of 0.1 Hz. Duplicate samples were measured for each sample type.

RESULTS AND DISCUSSION

Rheological Properties of Double Network Gels

he DN gel visco-elastic properties were studied by small deformation oscillatory rheology that is generally used to probe the system's internal interactions and gelling behavior. Using the method, we could see how the cross-linking affected the rheological properties of different samples. Cross-linking with either method did not greatly alter the loss tangent Tanδ (G″/G′) of WBE or catechol (**Supplementary Figures 1A,B**), yet from the moduli data of the samples (**Supplementary Figures 1C,D**) it is clear that *Th*L cross-linking affects the catechol system and it becomes a measurable fluid, i.e. a visco-elastic fluid (Tanδ above 1) with a clear response to frequency (**Supplementary Figure 1D**) showing a cross-over of G″ and G′ at around 0.55 Hz where G′

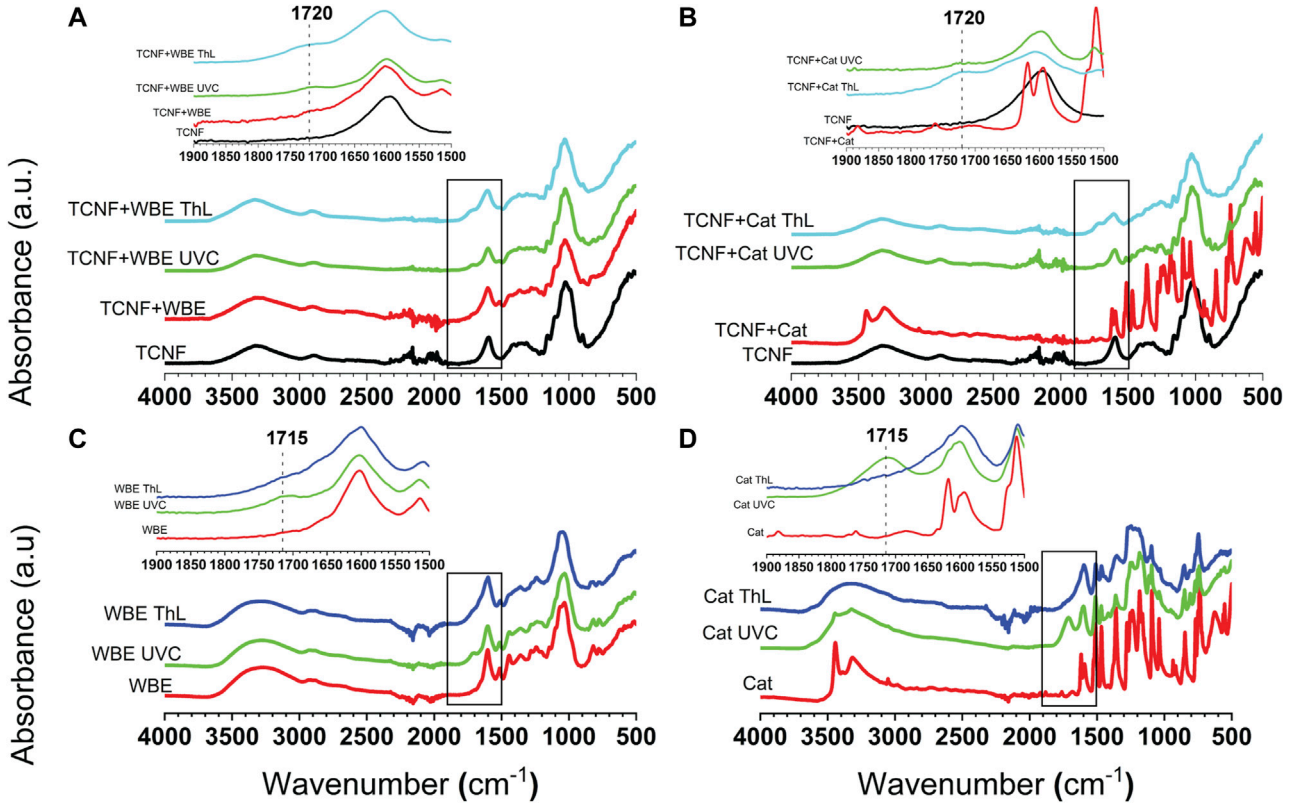

FIGURE 3 | FTIR spectra of the samples after different cross-linking methods and the corresponding untreated samples. **(A)** Willow bark extract (WBE) with TEMPO-oxidized cellulose nanofibrils (TCNF), **(B)** catechol (Cat) with TEMPO-oxidized cellulose nanofibrils (TCNF), **(C)** Willow bark extract (WBE), and **(D)** catechol (Cat). Inset spectra showing the boxed part of each spectrum to indicate peaks at 1720 cm^{-1} **(A,B)** and at 1715 cm^{-1} **(C,D)**.

becomes larger than G″. These changes in the catechol system indicate a change in the structure of the system due to cross-linking, i.e. polymerization. However, in the presence of TCNF, the cross-linking increased both G′ and G″ values (**Figures 2A–C**) and lowered the Tanδ values below 1 (**Supplementary Figures 2A–C**) indicating a greater increase in the elastic component of the system and leading to a more solid-like system, a gel. A clear change in the rheological behavior is observed as G′ is larger than G″ and the systems respond to frequency. These suggest increased amount of internal interactions in the gels that can be i) due to polymerization of the WBE/catechol and ii) their interactions with TCNF. In addition to the polymerization, the latter is suggested to take place in the system at least with TCNF and WBE as the moduli are increased and the Tanδ decreased even without cross-linking (**Figure 2A** brown line and **Supplementary Figure 2A** brown line). The cross-linking of the molecules of WBE and catechol led to a network of nanoparticles and large polymers visualized by AFM (**Supplementary Figure 3**) and analyzed by SEC (**Supplementary Figure 4**), respectively. The cross-linked WBE was effectively interlaced to TCNF network through non-covalent interactions with the abundant carboxylate groups (ATR-FT-IR spectra presented in **Figure 3** and discussed later). The combination of two chemically separate networks improved the strength of the hydrogel (Haque et al., 2012).

To further verify the interaction between WBE and TCNF without cross-linking, quartz crystal microbalance with dissipation monitoring (QCM-D) was used. From QCM-D it was evident that WBE adsorbed onto the TCNF surface, indicated by the negative change in frequency, and formed a tight and thin layer as dissipation did not change during adsorption (**Supplementary Figure 5**). Owing to the small negative charge in frequency (Δf = −5.5 Hz) of WBE adsorbing on TCNF thin film, the adsorbed amount was low, yet rinsing did not remove the adsorbed molecules, suggesting non-electrostatic interaction between WBE and TCNF.

In contrast, the catechol lowered the moduli of TCNF (**Figure 2A**, black line) and did not affect the Tanδ (**Supplementary Figure 2A**, black line) of the TCNF gel network before cross-linking and thus, can be considered not to interact with TCNF in the same manner as WBE. The cross-linking of the systems by UVC showed clearly that interactions within the system were increased (**Figure 2B**, **Supplementary Figure 2B**). The ratio of G' to G'' was increased and the Tanδ was lowered now for both the TCNF with WBE and TCNF with catechol (**Supplementary Figure 2C**). Similar effects were noticed for enzymatic cross-linking of TCNF with both WBE and catechol (**Figure 2C**, **Supplementary Figure 2C**). It is noteworthy to mention that the addition of the enzyme to TCNF alone affected negatively the TCNF gel network (**Figure 2C**; **Supplementary Figure 2C**). *Th*L can adsorb onto cellulose surface (Saarinen et al., 2009), and the result suggests

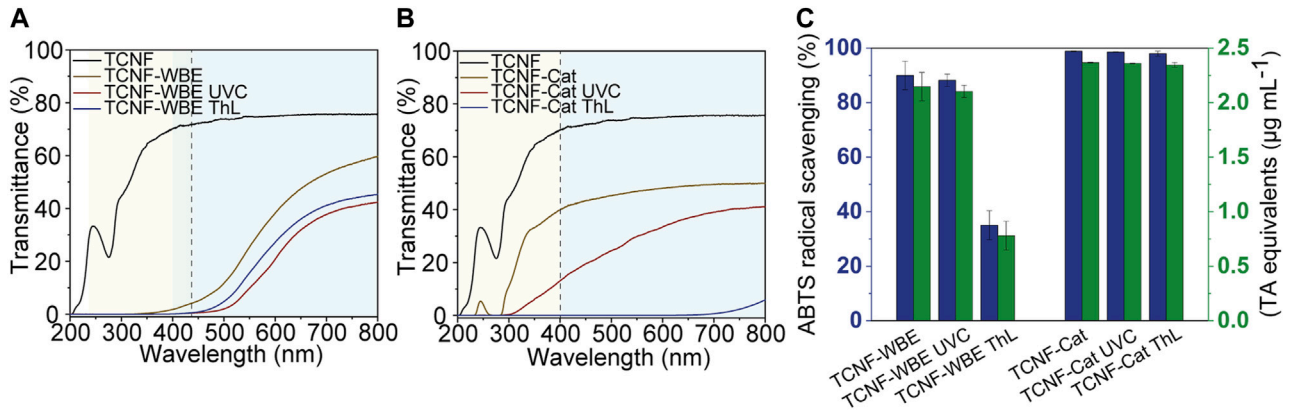

FIGURE 4 | UV-shielding properties of TEMPO-oxidized cellulose nanofibril (TCNF) nanocomposite films containing **(A)** willow bark extract (WBE) and **(B)** catechol (Cat). **(C)** The radical scavenging activity (blue bars) and tannic acid (TA) equivalents (green bars) of the nanocomposite films.

that even in small quantities this interaction can disrupt the interactions between fibrils in the TCNF network.

Bioactive Properties of Films

The double network hydrogels of TCNF with WBE or catechol were casted to nanocomposite films (**Scheme 1B**). The results showed that the suspension casted films of TCNF with WBE or catechol very effectively block both UVB (280–320 nm) and UVA (320–400 nm) irradiation (**Figures 4A,B**). The strong UV-absorbing capacity is a characteristic for natural polyphenols (Anouar et al., 2012). The effect was enhanced when WBE and catechol were cross-linked either by UVC or by *Th*L enzyme. TCNF-WBE films blocked all UV-light even without polymerization (**Figure 4A**), whereas in case of TCNF-catechol, only the enzymatically cross-linked film blocked UV completely (**Figure 4B**).

The difference in UV-blocking properties of TCNF-WBE and TCNF-catechol was most likely due to different initial polymer sizes. The initial polymer size was larger for WBE than for catechol (**Supplementary Figure 4**), which also affected the chromophore characteristics and light absorption ability. Increasing the polymer size can lead to a bathochromic shift toward darker color (IARC Working Group on the Evaluation of Carcinogenic Risks to Humans, 2010), which was evident for both WBE and catechol (**Supplementary Video 1**). The difference in the resulting polymer size can be due to different initial monomer size and cross-linking mechanism. Laccases catalyze oxidation of a broad variety of aromatic and nonaromatic substrates. During the reaction, the substrate molecule loses one electron and forms a highly reactive free radical, which can further undergo reactions, such as cross-linking of monomers (Claus, 2004). The use of laccases has been shown to be effective and ecological in applications such as pulp delignification, bioremediation of pollutants, and food processing (Riva, 2006). Although WBE contains (+)-catechin with similar *o*-phenol moieties as catechol, the position and size of substituents influence the ability of the substrate to bind to the laccase active site (Xu, 1996; D'Acunzo et al., 2002). In addition to (+)-catechin, WBE contains two other components, picein and triandrin (**Figure 1C**), which can presumably also react with laccases. The enzyme cross-linking of catechol in the presence of TCNF produced a material that completely blocked all wavelengths from 200 to 700 nm and only less than 10% of 700–800 nm light was passed through (**Figure 4B**). Depending on the cross-linking method, we were able to produce materials with selective light-adsorbing capacity ranging from total blocking of wavelengths below 700 nm (TCNF-catechol *Th*L) to TCNF-WBE that blocked only wavelengths below 400 nm. Previously, it has been shown that UV-protecting ability can be improved by increasing the concentration of polyphenols in the film (Li et al., 2019). The results presented here, however, showed that the UV-absorbing properties of polyphenols can be adjusted by controlling the extent of polymerization, rather than with increasing the concentration.

Free radicals, such as reactive oxygen species, cause damage to a wide variety of biomolecules and phenolic compounds capable of donating hydrogen atoms can suppress their formation (Choi et al., 2002). The skin defense mechanism against UV radiation, i.e., formation of melanin pigment, is also based on the redox and polymerization reactions of catecholic precursors, such as 3,4-dihydroxyphenylalanine (Sedõ et al., 2013). Herein, we found that the radical scavenging ability of the WBE and catechol in solutions was almost 100% (**Supplementary Figure 6B**). However, solutions are typically not feasible for use in radical scavenging and solid material embedded antioxidants are needed. Thus, using a nanocellulose-based material that can readily form thin films and a method to immobilize the radical scavenging molecules into the thin film (cross-linking) seem plausible. The radical scavenging activity of WBE and catechol polymerized together with a TCNF network was as high as the activity of the respective molecules in solution (**Figure 4C** vs. **Supplementary Figure 6B**). In time, if the WBE and catechol were not cross-linked, they were washed off from the TCNF films (**Supplementary Figure 7**). The leaching of plant extracts from materials is a well-acknowledged issue, which has been limiting their use (Tondi et al., 2013b). Chemical characteristics, such as higher molecular weight and number of hydroxyl substituents and aromatic rings, have been previously shown to improve the adsorption of phenolic compounds on cellulose (Phan et al., 2015). Based on visual assessment, cross-linking of WBE and catechol in the presence of a nanofibrillar network prevented the

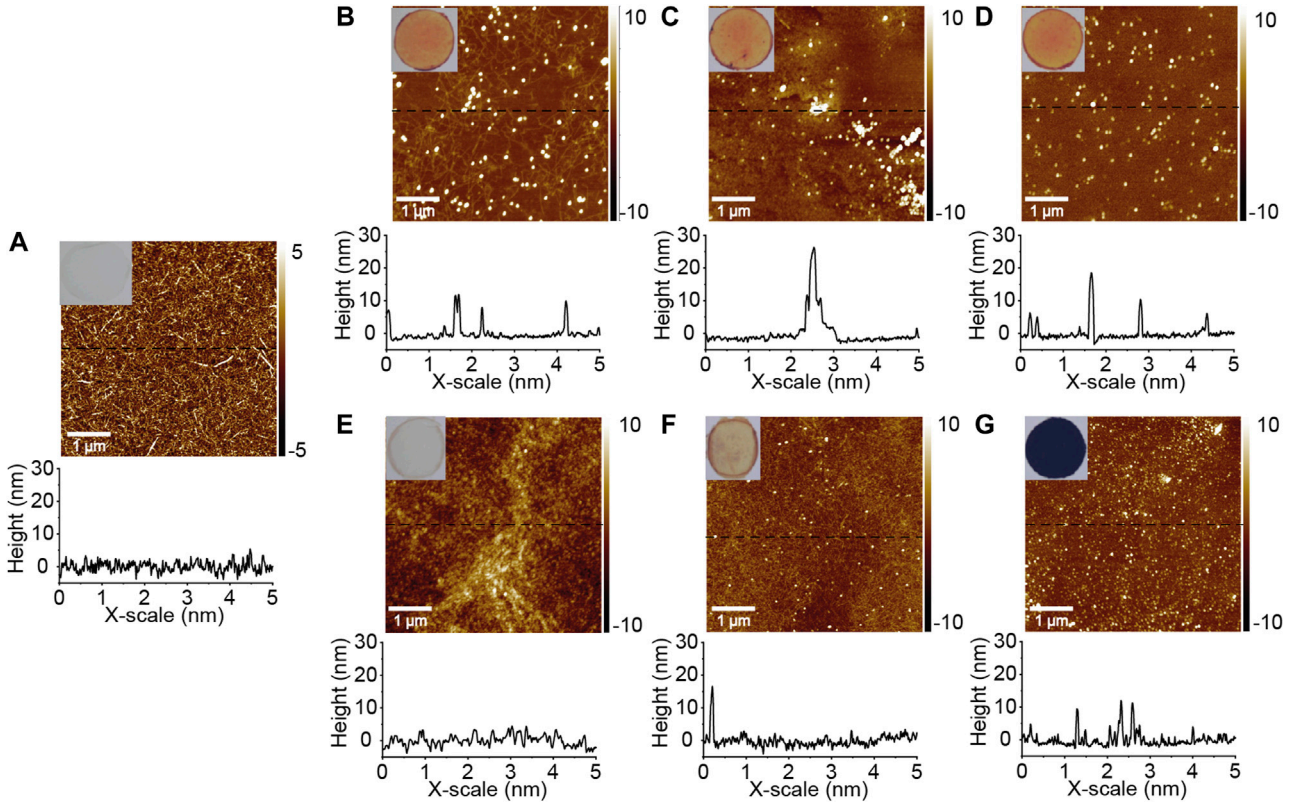

FIGURE 5 | Images of casted films, AFM height images, and cross-section profiles of corresponding spin-coated films. **(A)** TEMPO-oxidized cellulose nanofibrils, **(B)** TEMPO-oxidized cellulose nanofibrils with Willow bark extract, **(C)** TEMPO-oxidized cellulose nanofibrils with Willow bark extract cross-linked with UVC, **(D)** TEMPO-oxidized cellulose nanofibrils with Willow bark extract cross-linked with *Th*L enzyme, **(E)** TEMPO-oxidized cellulose nanofibrils with catechol, **(F)** TEMPO-oxidized cellulose nanofibrils with catechol cross-linked with UVC, **(G)** TEMPO-oxidized cellulose nanofibrils with catechol cross-linked with *Th*L enzyme.

color fading when immersed in water (**Supplementary Figure 7**). The cross-linking, however, did not prevent the materials' ability to scavenge radicals (**Figure 4C**). The enzymatic cross-linking of WBE lowered the radical scavenging ability from 90% to approximately 40%. The UV cross-linking, however, did not affect the radical scavenging ability of the molecules at all. Enzymatically crosslinked TCNF-WBE films had a poorer ability to block UV-light and a poorer ability to act as an antioxidant than the respective film crosslinked with UVC. Radical scavenging capacity of polyphenols correlates with the number of phenolic units having accessible hydroxyl groups and in addition, polymeric polyphenols can have lower antioxidant activity than smaller monomeric or dimeric products (Plumb et al., 1998; Bors and Michel, 1999). Therefore, the reduction in free radical scavenging was most likely due to the more effective polymerization of WBE with the enzyme, which lowered the number of accessible scavenging phenolic units, also observed as larger polymer size (**Supplementary Figure 4**).

Morphology of the Films

Atomic force microscopy (AFM) results in **Figure 5**, **Supplementary Figures 8–13** reveal that when the WBE was cross-linked in the presence of TCNF it formed nanoclusters or beads (**Figures 5C,D**, **Supplementary Figures 8, 9** respectively) in addition to polymeric fragments (**Supplementary Figure 4**). The WBE formed these nanoparticles also without cross-linking (**Figures 5B**; **Supplementary Figure 10**), but they were somewhat smaller (height approximately 10 nm) compared to the cross-linked ones (10–30 nm, **Figures 5C,D**, **Supplementary Figures 8, 9** respectively). The distribution of the particles within the TCNF matrix appeared to be more uniform with the enzyme cross-linking (**Figures 5D**, **Supplementary Figure 8**) and they were more even in size compared to the UVC cross-linked material (**Figures 5D**, **Supplementary Figure 8**). The AFM images for TCNF and catechol (**Figures 5E–G**, **Supplementary Figures 11–13**) showed that catechol formed nanoparticles only when it was cross-linked (**Figures 5F,G**, **Supplementary Figures 12, 13**). The nanoparticles were smaller in size compared to WBE particles and they were equally distributed within the TCNF matrix regardless of the cross-linking method. The TCNF sample showed only nanofibrils and nanoparticles similar to WBE and catechol samples were not seen (**Figure 5A** and **Supplementary Figure 14**). The TCNF sample surface was evenly covered with the fibrils.

Chemical and Mechanical Properties of Films

From the Fourier-transform infrared (FTIR) results shown in **Figure 3** it can be observed that no covalent bonding between

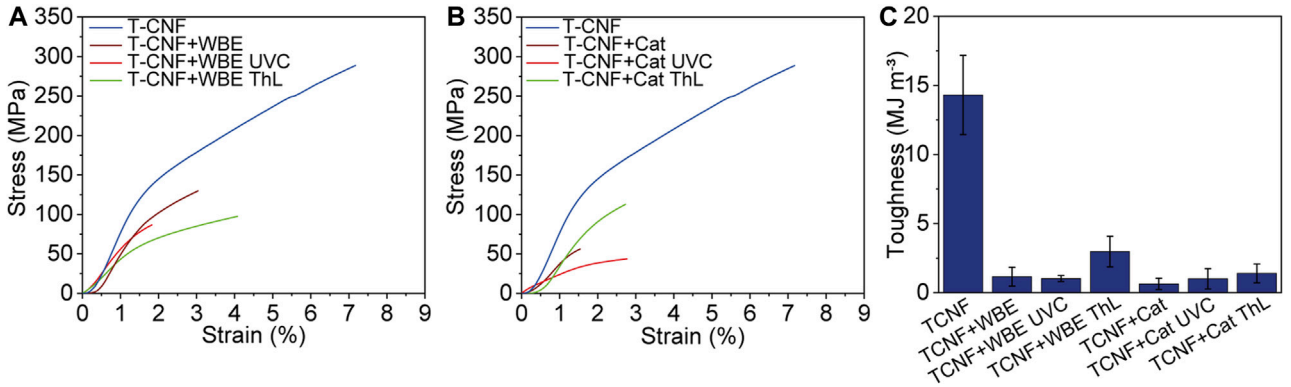

FIGURE 6 | Tensile stress–strain curves of **(A)** willow bark extract (WBE) and **(B)** catechol (Cat) containing TEMPO-oxidized cellulose nanofibril (TCNF) films with and without UVC and *Th*L cross-linking, and **(C)** toughness of the corresponding films.

TCNF and WBE or catechol occurred. Thus, the entrapment of WBE and catechol by cross-linking in the TCNF matrix was most probably due to formation of polymeric particles and fragments and their cross-linking via polymerization, which formed a double network hydrogel where TCNF offered a structural network guiding the formation of WBE/catechol nanoparticle network.

TCNF FTIR spectrum showed typical peaks of native cellulose (υOH 3,600–3,100 cm^{-1}, υCH 2,901, 1,431 cm^{-1}, υH_2 O 1641 cm^{-1}, υC-O 1165 cm^{-1}, 1,059 cm^{-1}, υCH2 899 cm^{-1}) (Ciolacu et al., 2011) and υC = O of sodium carboxylate at 1,603 cm^{-1} (Fujisawa et al., 2011). UVC and *Th*L did not cause chemical changes in pure TCNF (**Supplementary Figure 5**). The FTIR spectra of WBE and catechol containing films, except untreated TCNF-catechol film (**Figure 3B** red line), were similar to pure TCNF film. A noteworthy difference was that the bands between 1,520 and 1,200 cm^{-1} were broader in WBE and catechol containing films owing to the overlapping absorption bands of aromatic rings in WBE and catechol with cellulose CH and CO stretches (Ricci et al., 2015). In addition, shoulder at approximately 1720 cm^{-1} was present in WBE and catechol containing TCNF films (A and B insets respectively), and could be attributed to protonated carboxyl groups of TCNF due to the addition of slightly acidic WBE and catechol (Jiang and Hsieh, 2016). The FTIR spectrum of pure WBE (**Figure 3C**) shows characteristic bands of polyphenol (υ_{OH} 3,300 cm^{-1}, υ_{CH} 2,930 cm^{-1}, $\upsilon_{arom.}$ 1,600–1,400 cm^{-1}, $\upsilon_{C\ O}$ 1,050 cm^{-1}) (Chupin et al., 2013). Cross-linking with UVC and *Th*L induced structural changes in aqueous solutions of WBE and catechol (**Figures 3C,D**). The structural changes in catechol caused either by UVC or by *Th*L enzyme were mere clear and larger compared to WBE. Similar features in the spectra of catechol and polymerized catechol that are shown in **Figure 3D** have been presented in the literature (Aktaş et al., 2003). During polymerization, monomeric units of catechol were condensed via C-C and C-O-C linkages, which could be observed as changes at $\upsilon_{C\text{-}C}$, $\upsilon_{C\text{-}H\text{-}arom.}$ 1,585, 1,510, 820–690 cm^{-1} and $\upsilon_{C\text{-}O\text{-}C}$ 1170, 1,280 cm^{-1} (Dubey et al., 1998). Both UVC cross-linked aqueous WBE and catechol showed a band at 1715 cm^{-1}, which was not present in *Th*L cross-linked aqueous solutions of WBE and catechol or untreated films with WBE and catechol. This result suggests that the cross-linking reactions triggered by UVC yielded a final polymeric product with a slightly different structure and molecular weight compared to enzymatic cross-linking. Owing to applied extraction conditions and auto-oxidation of polyphenols, compared with catechol, WBE contained larger oligomeric and polymeric structures before the enzymatic or UVC cross-linking and therefore, the observed structural changes were not as large as with catechol, which was present as a monomer prior to cross-linking (**Supplementary Figures 3, 4**) (Tanaka et al., 2010). The possible interfacial interactions, namely different hydrogen bonding of WBE molecules with C-H and O-H groups on the TCNF fibrils' surfaces, were physical by nature. Being a bulk method, FTIR is not sensitive to probing the interactions occurring at the material's surface only, but the result is an average of a larger sample volume, thus showing only weak peaks for the changes happening due to surface reactions.

Tensile testing of the films showed that the addition of WBE or catechol or their cross-linking affected negatively the mechanical performance of dried TCNF films (**Figures 6A–C**). Here, the reported tensile strength of pure TCNF was slightly higher than that reported elsewhere (233 MPa, elongation 7.6% (Fukuzumi et al., 2009)) due to small size of specimen, which is known to influence the observed tensile properties (Hervy et al., 2017). However, the comparison between different samples could be carried out, keeping the specimen measures constant. The strain and toughness of the dry films were significantly lowered by the addition of WBE or catechol and polymerization made the dry films more brittle. This could be caused by the polymeric matrix disturbing the cellulose–cellulose interactions that usually form upon drying of the system as the polymeric matrix has been formed in the hydrogel state around and in between the fibrils. When the DN hydrogel was dried, the WBE/catechol polymer matrix prevented the formation of interfibrillar interactions making the films more brittle. A similar trend in reduction of tensile properties has been reported in the literature for other tannins containing cellulose films (Olejar et al., 2014; Missio et al.,

TABLE 1 | Oxygen transmission rates (OTR) of TEMPO-oxidized cellulose nanofibril (TCNF) film, TCNF film with willow bark extract (WBE) (TCNF-WBE), and TCNF film treated with catechol (TCNF-Cat) untreated, UVC-treated, or *Th*L enzyme treated at relative humidity 50%, and the film thicknesses.

Film	OTR (cc/m^{2}day)	Thickness (μm)
TCNF	4.45 ± 5.18	24.3 ± 1.5
TCNF-WBE	0.90 ± 3.12	85.3 ± 2.5
TCNF-WBE UVC	3.43 ± 1.57	74.0 ± 3.6
TCNF-WBE *Th*L	1.63 ± 1.75	46.0 ± 1.7
TCNF-Cat	9.68 ± 5.88	50.7 ± 1.2
TCNF-Cat UVC	4.30 ± 0.23	51.0 ± 7.2
TCNF-Cat *Th*L	n.d.[a]	57.3 ± 3.5

[a]*The sample was too fragile to be measured.*

2018). The distribution of WBE and catechol particles was most even in the *Th*L cross-linked samples (**Figures 5C,F** respectively), which could plausibly explain the slightly better tensile toughness values of *Th*L cross-linked TCNF-WBE and TCNF-catechol films (**Figure 6C**). The aggregation of nanoparticles typically has a negative influence on the mechanical strength of polymer composite films (Olsson et al., 2010). The mechanical performance of the self-standing films could be increased by increasing the amount of materials in the film or by depositing the film on a support structure. In applications such as barrier coatings in packaging the barrier coating serves as a thin coating layer in between other functional barrier coatings (Wang et al., 2018). This would be an ideal way of applying a barrier layer such as the one described in this study.

The oxygen transmission rates (OTR) of the different films are shown in **Table 1** along with the film thicknesses. The thickness of pure TCNF was at least half of the thickness of the other films. This was due to lower total solids content of the pure TCNF solution from which the films were casted. The amount of TCNF was kept constant for all solutions used to prepare films; however, the amount of added cross-linker contributed to the total solids content of the solutions and thus, to the resulting film thickness.

The thickness difference in WBE and catechol containing films can be mainly explained with the different sizes of oligomeric products. However, although *Th*L cross-linked WBE has the largest polymer size according to SEC results (**Supplementary Figure 4**), the thickness of the *Th*L cross-linked TCNF-WBE film was almost half of the same films with and without UVC cross-linking. This suggests that in the *Th*L cross-linked TCNF-WBE film, the constituents can be packed closer together resulting in a denser material. In TCNF-catechol films, the variance in the thickness was relatively small. The thickness remained the same in uncross-linked and UVC cross-linked TCNF-catechol films. With *Th*L cross-linking, the thickness increased slightly, most likely owing to the bigger size of cross-linked polycatechols. In general, nanocellulose films exhibit excellent oxygen barrier properties since the compact network formed by hydrogen bonding interconnected fibrils physically prevents the permeation of oxygen molecules (Syverud and Stenius, 2009). The values in **Table 1** show that all films had good/excellent oxygen barrier properties since the oxygen transmission rates (OTR) varied between 1–10 cc/m^{2}day (Abdellatief and Welt, 2013). The OTR values for pure TCNF films have been reported to vary from 1.65×10^{-3} cc/m^{2}day to 13.5 cc/m^{2}day at RH 35 and 100%, respectively (Qing et al., 2013). The addition of WBE and catechol with and without cross-linking yielded somewhat lower to similar oxygen transmission rates as neat TCNF. And exception was TCNF film with catechol without any cross-linking. The size and distribution of entrapped WBE and catechol particles varied depending on the cross-linking mechanism. The interaction of two physically interlaced networks of TCNF and WBE or catechol could plausibly yield to changes in the compactness of the films, i.e., number of pores and voids induced by polymerization. The WBE on its own already interacted with TCNF (**Figure 2A**, **Supplementary Figure 2A**) and increased the surface roughness (**Figure 4B**) creating a less dense film and thus, leading to lower OTR. Cross-linking this with UVC created a less evenly distributed hydrogel network of nanoparticles (**Figure 5C**) increasing the OTR. The enzyme cross-linking caused increase in interactions (**Figure 2C**) and a more homogeneous distribution of smaller particles (**Figure 5D**), which in turn lowered the surface roughness and the OTR as a more connected network was created. The catechol alone did not interact with the TCNF network (**Figure 2A**, **Supplementary Figure 2A**) and OTR was clearly higher than in TCNF. The UVC cross-linking of the TCNF film with catechol decreased the OTR compared to non-cross-linked TCNF film with catechol indicating that increased connectivity of the network translated into a less porous film. The OTR value of UVC cross-linked TCNF with catechol film was comparable to TCNF alone suggesting that the interaction between fibrils that the catechol without cross-linking disturbed were replaced by interactions of polymerized catechol after UVC treatment. Unfortunately, we were not able to measure the OTR for the enzyme cross-linked TCNF-catechol film, as it was very fragile despite added sorbitol as a plasticizer. This suggests that even though the chemical structures of UVC and *Th*L cross-linked TCNF-catechol films were similar, the arrangement of polymeric particles and interaction with the TCNF network was notably deviating, most likely owing to the different mechanisms of enzymatic and photo-induced cross-linking.

CONCLUSION

In this work, we showed that natural polyphenols from willow bark can be embedded in a nanocellulose matrix via double network hydrogel formation in a way that the bioactive properties (UV-vis adsorption and antioxidant nature) of the polyphenols could be transferred to the resulting bionanocomposite material. In contrast to earlier efforts regarding double network (DN) hydrogels that rely on synthetic polymers and chemical initiators, cross-linking of polyphenols was carried out with nonhazardous, simple, and green methods using UV irradiation or enzymatic catalysis. The rheological investigation of the DN hydrogels showed that the formation of the second network increased the amount of interactions in the system and increased the hydrogel rheological properties. Rheology also showed differences between the cross-linking methods and the interactions within the different systems. Willow bark extract (WBE) appeared to be able to interact with the

TEMPO-oxidized nanocellulose network (TCNF) even without cross-linking, whereas catechol employed as a model molecule did not cause significant differences in the TCNF network without cross-linking. The morphological analysis revealed that both UV irradiation and enzymatic cross-linking resulted in a polymeric nanoparticle network with different structures and interaction with the TCNF network, and thus to nanocomposite films with altering physical and chemical properties. The nanocellulose network appeared to guide the formation of the polyphenol nanoparticle network and the resulting system was best described as a double network hydrogel bionanocomposite. The resulting films had varying UV blocking and radical scavenging capacities depending on the applied cross-linking method. This observed tunability enabled adjusting the bioactive properties with more raw material efficient means, as increasing the concentration of the bioactive molecule above 0.8 wt% was not required. The excellent OTR values of CNF materials were not compromised due to the addition of the bioactive compound and in some cases even slightly increased compared to TCNF film. Overall, the fully wood-based material introduced in this study prepared by tunable mild cross-linking methods serves as a proof of concept material. The DN hydrogels presented here could have potential in different applications where nontoxic, biodegradable, and biobased hydrogel materials are needed for example in pharmaceutical, medical, and food applications. The composite films prepared from the DN hydrogels have potential as barrier-coating layers with bioactive properties in applications where oxygen barriers, light guidance, and specific adsorption are required. The most potential application is in food and pharmaceutical packaging.

DATA AVAILABILITY STATEMENT

The original contributions presented in the study are included in the article/**Supplementary Material**, further inquiries can be directed to the corresponding author.

AUTHOR CONTRIBUTIONS

TL performed most of the experiments and provided the first draft of the manuscript. RG performed QCM-D experiment and MÖ helped with the data analysis. SA and PL helped to analyze the data and wrote sections of the manuscript. All authors contributed to manuscript revision, read, and approved the submitted version. SA supervised the research and planned the experiments together with TL. TL, SA and PL prepared figures.

FUNDING

The work has been conducted under Academy of Finland's project #326262/#311608, #327209, and #327195.

ACKNOWLEDGMENTS

The authors thank Martina Blomster-Andberg for providing the laccase enzyme, Leena Pitkänen with assistance on size exclusion chromatography, and Hille Rautkoski for measuring the oxygen transmission rates for the films. We also thank Aalto University Department of Biosystems and Bioproducts for funding the research. We are grateful for the support by the FinnCERES Materials Bioeconomy Ecosystem and the Bioeconomy infrastructure on the Otaniemi campus.

SUPPLEMENTARY MATERIAL

The Supplementary Material for this article can be found online at: https://www.frontiersin.org/articles/10.3389/fceng.2021.708170/full#supplementary-material

Supplementary Material contains the following data and information: 1) Rheological behavior of willow bark extract and catechol, 2) Tanδ values of TCNF materials with and without WBE or catechol, 3) AFM images of WBE and catechol with and without UVC- and laccase treatment, 4) SEC data of aqueous WBE and catechol solutions, 5) QCM-D adsorption data for WBE on TEMPO-CNF thin-film, 6) Tannic acid calibration curve and antioxidant activity of pure TEMPO-CNF, WBE, and catechol, 7) Photographs of different films before and after immersing in water, 8) FTIR spectra of TEMPO-CNF film with and without UVC- and laccase treatment, 9) video of laccase reaction with WBE and catechol.

REFERENCES

Abd El-Rehim, H. A. (2006). Characterization and Possible Agricultural Application of Polyacrylamide/sodium Alginate Crosslinked Hydrogels Prepared by Ionizing Radiation. *J. Appl. Polym. Sci.* 101, 3572–3580. doi:10.1002/app.22487

Abdellatief, A., and Welt, B. A. (2013). Comparison of New Dynamic Accumulation Method for Measuring Oxygen Transmission Rate of Packaging against the Steady-State Method Described by ASTM D3985. *Packag. Technol. Sci.* 26, 281–288. doi:10.1002/pts.1974

Abe, K., Iwamoto, S., and Yano, H. (2007). Obtaining Cellulose Nanofibers with a Uniform Width of 15 Nm from wood. *Biomacromolecules* 8, 3276–3278. doi:10.1021/bm700624p

Ajao, O., Benali, M., Faye, A., Li, H., Maillard, D., and Ton-That, M. T. (2021). Multi-product Biorefinery System for wood-barks Valorization into Tannins Extracts, Lignin-Based Polyurethane Foam and Cellulose-Based Composites: Techno-Economic Evaluation. *Ind. Crops Prod.* 167, 113435. doi:10.1016/j.indcrop.2021.113435

Aktaş, N., Şahiner, N., Kantoğlu, Ö., Salih, B., and Tanyolaç, A. (2003). Biosynthesis and Characterization of Laccase Catalyzed Poly(Catechol). *J. Polym. Environ.* 11, 123–128. doi:10.1023/A:1024639231900

Altemimi, A., Lakhssassi, N., Baharlouei, A., Watson, D., and Lightfoot, D. (2017). Phytochemicals: Extraction, Isolation, and Identification of Bioactive Compounds from Plant Extracts. *Plants* 6, 42. doi:10.3390/plants6040042

Anouar, E. H., Gierschner, J., Duroux, J.-L., and Trouillas, P. (2012). UV/Visible Spectra of Natural Polyphenols: A Time-dependent Density Functional Theory Study. *Food Chem.* 131, 79–89. doi:10.1016/j.foodchem.2011.08.034

Bechtold, T., Turcanu, A., Ganglberger, E., and Geissler, S. (2003). Natural Dyes in Modern Textile Dyehouses - How to Combine Experiences of Two Centuries to Meet the Demands of the Future? *J. Clean. Prod.* 11, 499–509. doi:10.1016/S0959-6526(02)00077-X

Bhattacharya, M., Malinen, M. M., Lauren, P., Lou, Y.-R., Kuisma, S. W., Kanninen, L., et al. (2012). Nanofibrillar Cellulose Hydrogel Promotes Three-Dimensional Liver Cell Culture. *J. Controlled Release* 164, 291–298. doi:10.1016/j.jconrel.2012.06.039

Bors, W., and Michel, C. (1999). Antioxidant Capacity of Flavanols and Gallate Esters: Pulse Radiolysis Studies. *Free Radic. Biol. Med.* 27, 1413–1426. doi:10.1016/S0891-5849(99)00187-2

Brglez Mojzer, E., Knez Hrnčič, M., Škerget, M., Knez, Ž., and Bren, U. (2016). Polyphenols: Extraction Methods, Antioxidative Action, Bioavailability and Anticarcinogenic Effects. *Molecules* 21, 901. doi:10.3390/molecules21070901

Chen, Q., Chen, H., Zhu, L., and Zheng, J. (2015). Fundamentals of Double Network Hydrogels. *J. Mater. Chem. B* 3, 3654–3676. doi:10.1039/c5tb00123d

Choi, C. W., Kim, S. C., Hwang, S. S., Choi, B. K., Ahn, H. J., Lee, M. Y., et al. (2002). Antioxidant Activity and Free Radical Scavenging Capacity between Korean Medicinal Plants and Flavonoids by Assay-Guided Comparison. *Plant Sci.* 163, 1161–1168. doi:10.1016/S0168-9452(02)00332-1

Chupin, L., Motillon, C., Charrier-El Bouhtoury, F., Pizzi, A., and Charrier, B. (2013). Characterisation of Maritime pine (*Pinus pinaster*) Bark Tannins Extracted under Different Conditions by Spectroscopic Methods, FTIR and HPLC. *Ind. Crops Prod.* 49, 897–903. doi:10.1016/j.indcrop.2013.06.045

Ciolacu, D., Ciolacu, F., and Popa, V. I. (2011). Amorphous Cellulose - Structure and Characterization. *Cellul. Chem. Technol.* 45, 13–21. Available at: https://www.cellulosechemtechnol.ro/pdf/CCT1-2(2011)/p.13-21.pdf.

Claus, H. (2004). Laccases: Structure, Reactions, Distribution. *Micron* 35, 93–96. doi:10.1016/j.micron.2003.10.029

Covington, A. D. (1997). Modern Tanning Chemistry. *Chem. Soc. Rev.* 26, 111–126. doi:10.1039/cs9972600111

D'Acunzo, F., Galli, C., and Masci, B. (2002). Oxidation of Phenols by Laccase and Laccase-Mediator Systems. Solubility and Steric Issues. *Eur. J. Biochem.* 269, 5330–5335. doi:10.1046/j.1432-1033.2002.03256.x

De France, K. J., Hoare, T., and Cranston, E. D. (2017). Review of Hydrogels and Aerogels Containing Nanocellulose. *Chem. Mater.* 29, 4609–4631. doi:10.1021/acs.chemmater.7b00531

Delgado-Sánchez, C., Letellier, M., Fierro, V., Chapuis, H., Gérardin, C., Pizzi, A., et al. (2016). Hydrophobisation of Tannin-Based Foams by Covalent Grafting of Silanes. *Ind. Crops Prod.* 92, 116–126. doi:10.1016/j.indcrop.2016.08.002

Dou, J., Xu, W., Koivisto, J. J., Mobley, J. K., Padmakshan, D., Kögler, M., et al. (2018). Characteristics of Hot Water Extracts from the Bark of Cultivated Willow (Salix sp.). *ACS Sust. Chem. Eng.* 6, 5566–5573. doi:10.1021/acssuschemeng.8b00498

Drury, J. L., and Mooney, D. J. (2003). Hydrogels for Tissue Engineering: Scaffold Design Variables and Applications. *Biomaterials* 24, 4337–4351. doi:10.1016/S0142-9612(03)00340-5

Dubey, S., Singh, D., and Misra, R. A. (1998). Enzymatic Synthesis and Various Properties of Poly(catechol). *Enzyme Microb. Tech.* 23, 432–437. doi:10.1016/S0141-0229(98)00063-5

Feng, S., Cheng, S., Yuan, Z., Leitch, M., and Xu, C. (2013). Valorization of Bark for Chemicals and Materials: A Review. *Renew. Sust. Energ. Rev.* 26, 560–578. doi:10.1016/j.rser.2013.06.024

Fujisawa, S., Okita, Y., Fukuzumi, H., Saito, T., and Isogai, A. (2011). Preparation and Characterization of TEMPO-Oxidized Cellulose Nanofibril Films with Free Carboxyl Groups. *Carbohydr. Polym.* 84, 579–583. doi:10.1016/j.carbpol.2010.12.029

Fukuzumi, H., Saito, T., Iwata, T., Kumamoto, Y., and Isogai, A. (2009). Transparent and High Gas Barrier Films of Cellulose Nanofibers Prepared by TEMPO-Mediated Oxidation. *Biomacromolecules* 10, 162–165. doi:10.1021/bm801065u

Gong, J. P. (2010). Why Are Double Network Hydrogels So Tough? *Soft Matter* 6, 2583–2590. doi:10.1039/b924290b

Haque, M. A., Kurokawa, T., and Gong, J. P. (2012). Super Tough Double Network Hydrogels and Their Application as Biomaterials. *Polymer* 53, 1805–1822. doi:10.1016/j.polymer.2012.03.013

Hervy, M., Santmarti, A., Lahtinen, P., Tammelin, T., and Lee, K.-Y. (2017). Sample Geometry Dependency on the Measured Tensile Properties of Cellulose Nanopapers. *Mater. Des.* 121, 421–429. doi:10.1016/j.matdes.2017.02.081

Hoare, T. R., and Kohane, D. S. (2008). Hydrogels in Drug Delivery: Progress and Challenges. *Polymer* 49, 1993–2007. doi:10.1016/j.polymer.2008.01.027

Hu, Z., Berry, R. M., Pelton, R., and Cranston, E. D. (2017). One-Pot Water-Based Hydrophobic Surface Modification of Cellulose Nanocrystals Using Plant Polyphenols. *ACS Sust. Chem. Eng.* 5, 5018–5026. doi:10.1021/acssuschemeng.7b00415

Hubbe, M. A., Ferrer, A., Tyagi, P., Yin, Y., Salas, C., Pal, L., et al. (2017). Nanocellulose in Thin Films, Coatings, and Plies for Packaging Applications: A Review. *BioResources* 12, 1. doi:10.15376/biores.12.1.2143-2233

IARC Working Group on the Evaluation of Carcinogenic Risks to Humans (2010). "General Introduction to the Chemistry of Dyes," in *Some Aromatic Amines, Organic Dyes, and Related Exposures*. Editor J. Daniel (Lyon, FR: International Agency for Research on Cancer), 55–67.

Isogai, A., Saito, T., and Fukuzumi, H. (2011). TEMPO-oxidized Cellulose Nanofibers. *Nanoscale* 3, 71–85. doi:10.1039/c0nr00583e

Jiang, F., and Hsieh, Y.-L. (2016). Self-assembling of TEMPO Oxidized Cellulose Nanofibrils as Affected by Protonation of Surface Carboxyls and Drying Methods. *ACS Sust. Chem. Eng.* 4, 1041–1049. doi:10.1021/acssuschemeng.5b01123

Kaiser, K., Schmid, M., and Schlummer, M. (2018). Recycling of Polymer-Based Multilayer Packaging: A Review. *Recycling* 3, 1. doi:10.3390/recycling3010001

Li, A.-N., Li, S., Zhang, Y.-J., Xu, X.-R., Chen, Y.-M., and Li, H.-B. (2014). Resources and Biological Activities of Natural Polyphenols. *Nutrients* 6, 6020–6047. doi:10.3390/nu6126020

Li, P., Sirviö, J. A., Haapala, A., Khakalo, A., and Liimatainen, H. (2019). Anti-oxidative and UV-Absorbing Biohybrid Film of Cellulose Nanofibrils and Tannin Extract. *Food Hydrocolloids* 92, 208–217. doi:10.1016/j.foodhyd.2019.02.002

Lohtander, T., Arola, S., and Laaksonen, P. (2019). Biomordanting Willow Bark Dye on Cellulosic Materials. *Coloration Technol.* 136, 3–14. doi:10.1111/cote.12442

Missio, A. L., Mattos, B. D., Ferreira, D. d. F., Magalhães, W. L. E., Bertuol, D. A., Gatto, D. A., et al. (2018). Nanocellulose-tannin Films: From Trees to Sustainable Active Packaging. *J. Clean. Prod.* 184, 143–151. doi:10.1016/j.jclepro.2018.02.205

Moubarik, A., Pizzi, A., Allal, A., Charrier, F., and Charrier, B. (2009). Cornstarch and Tannin in Phenol-Formaldehyde Resins for Plywood Production. *Ind. Crops Prod.* 30, 188–193. doi:10.1016/j.indcrop.2009.03.005

Olejar, K. J., Ray, S., Ricci, A., and Kilmartin, P. A. (2014). Superior Antioxidant Polymer Films Created through the Incorporation of Grape Tannins in Ethyl Cellulose. *Cellulose* 21, 4545–4556. doi:10.1007/s10570-014-0447-4

Olsson, R. T., Azizi Samir, M. A. S., Salazar-Alvarez, G., Belova, L., Ström, V., Berglund, L. A., et al. (2010). Making Flexible Magnetic Aerogels and Stiff Magnetic Nanopaper Using Cellulose Nanofibrils as Templates. *Nat. Nanotech* 5, 584–588. doi:10.1038/nnano.2010.155

Pásztory, Z., Mohácsiné, I. R., Gorbacheva, G., and Börcsök, Z. (2016). The Utilization of Tree Bark. *BioRes.* 11, 7859–7888. doi:10.15376/biores.11.3.Pasztory

Phan, A. D. T., Netzel, G., Wang, D., Flanagan, B. M., D'Arcy, B. R., and Gidley, M. J. (2015). Binding of Dietary Polyphenols to Cellulose: Structural and Nutritional Aspects. *Food Chem.* 171, 388–396. doi:10.1016/j.foodchem.2014.08.118

Pietarinen, S. P., Willför, S. M., Ahotupa, M. O., Hemming, J. E., and Holmbom, B. R. (2006). Knotwood and Bark Extracts: Strong Antioxidants from Waste Materials. *J. Wood Sci.* 52, 436–444. doi:10.1007/s10086-005-0780-1

Plumb, G. W., De Pascual-Teresa, S., Santos-Buelga, C., Cheynier, V., and Williamson, G. (1998). Antioxidant Properties of Catechins and Proanthocyanidins: Effect of Polymerisation, Galloylation and Glycosylation. *Free Radic. Res.* 29, 351–358. doi:10.1080/10715769800300391

Qing, Y., Sabo, R., Cai, Z., and Wu, Y. (2013). Resin Impregnation of Cellulose Nanofibril Films Facilitated by Water Swelling. *Cellulose* 20, 303–313. doi:10.1007/s10570-012-9815-0

Quideau, S., Deffieux, D., Douat-Casassus, C., and Pouységu, L. (2011). Plant Polyphenols: Chemical Properties, Biological Activities, and Synthesis. *Angew. Chem. Int. Ed.* 50, 586–621. doi:10.1002/anie.201000044

Re, R., Pellegrini, N., Proteggente, A., Pannala, A., Yang, M., and Rice-Evans, C. (1999). Antioxidant Activity Applying an Improved ABTS Radical Cation Decolorization Assay. *Free Radic. Biol. Med.* 26, 1231–1237. doi:10.1016/S0891-5849(98)00315-3

Ricci, A., Olejar, K. J., Parpinello, G. P., Kilmartin, P. A., and Versari, A. (2015). Application of Fourier Transform Infrared (FTIR) Spectroscopy in the Characterization of Tannins. *Appl. Spectrosc. Rev.* 50, 407–442. doi:10.1080/05704928.2014.1000461

Rittstieg, K., Suurnakki, A., Suortti, T., Kruus, K., Guebitz, G., and Buchert, J. (2002). Investigations on the Laccase-Catalyzed Polymerization of Lignin Model Compounds Using Size-Exclusion HPLC. *Enzyme Microb. Tech.* 31, 403–410. doi:10.1016/S0141-0229(02)00102-3

Riva, S. (2006). Laccases: Blue Enzymes for green Chemistry. *Trends Biotechnol.* 24, 219–226. doi:10.1016/j.tibtech.2006.03.006

Saarinen, T., Orelma, H., Grönqvist, S., Andberg, M., Holappa, S., and Laine, J. (2009). Adsorption of Different Laccases on Cellulose and Lignin Surfaces. *BioResources* 4, 94–110. doi:10.15376/biores.4.1.94-110

Saito, T., Kimura, S., Nishiyama, Y., and Isogai, A. (2007). Cellulose Nanofibers Prepared by TEMPO-Mediated Oxidation of Native Cellulose. *Biomacromolecules* 8, 2485–2491. doi:10.1021/bm0703970

Sánchez-Martín, J., Beltrán-Heredia, J., and Gibello-Pérez, P. (2011). Adsorbent Biopolymers from Tannin Extracts for Water Treatment. *Chem. Eng. J.* 168, 1241–1247. doi:10.1016/j.cej.2011.02.022

Sedó, J., Saiz-Poseu, J., Busqué, F., and Ruiz-Molina, D. (2013). Catechol-based Biomimetic Functional Materials. *Adv. Mater.* 25, 653–701. doi:10.1002/adma.201202343

Shi, M., Nie, Y., Zheng, X.-Q., Lu, J.-L., Liang, Y.-R., and Ye, J.-H. (2016). Ultraviolet B (UVB) Photosensitivities of tea Catechins and the Relevant Chemical Conversions. *Molecules* 21, 1345. doi:10.3390/molecules21101345

Solano, F. (2014). Melanins: Skin Pigments and Much More-Types, Structural Models, Biological Functions, and Formation Routes. *New J. Sci.* 2014, 1–28. doi:10.1155/2014/498276

Syverud, K., and Stenius, P. (2009). Strength and Barrier Properties of MFC Films. *Cellulose* 16, 75–85. doi:10.1007/s10570-008-9244-2

Tanaka, T., Matsuo, Y., and Kouno, I. (2010). Chemistry of Secondary Polyphenols Produced during Processing of tea and Selected Foods. *Ijms* 11, 14–40. doi:10.3390/ijms11010014

Tondi, G., Schnabel, T., Wieland, S., and Petutschnigg, A. (2013a). Surface Properties of Tannin Treated wood during Natural and Artificial Weathering. *Int. Wood Prod. J.* 4, 150–157. doi:10.1179/2042645313Y.0000000047

Tondi, G., Thevenon, M. F., Mies, B., Standfest, G., Petutschnigg, A., and Wieland, S. (2013b). Impregnation of Scots pine and Beech with Tannin Solutions: Effect of Viscosity and wood Anatomy in wood Infiltration. *Wood Sci. Technol.* 47, 615–626. doi:10.1007/s00226-012-0524-5

Torreggiani, A., Jurasekova, Z., Sanchez-Cortes, S., and Tamba, M. (2008). Spectroscopic and Pulse Radiolysis Studies of the Antioxidant Properties of (+)catechin: Metal Chelation and Oxidizing Radical Scavenging. *J. Raman Spectrosc.* 39, 265–275. doi:10.1002/jrs.1849

Tsao, R., and Deng, Z. (2004). Separation Procedures for Naturally Occurring Antioxidant Phytochemicals. *J. Chromatogr. B* 812, 85–99. doi:10.1016/j.jchromb.2004.09.02810.1016/s1570-0232(04)00764-0

Wang, J., Gardner, D. J., Stark, N. M., Bousfield, D. W., Tajvidi, M., and Cai, Z. (2018). Moisture and Oxygen Barrier Properties of Cellulose Nanomaterial-Based Films. *ACS Sust. Chem. Eng.* 6, 49–70. doi:10.1021/acssuschemeng.7b03523

Wang, Y., Qi, X., Zhang, Z., and Pang, J. (2021). A Facile and Efficient Universal Strategy of Superhydrophobic Materials Based on Plant Polyphenols as Multifunctional Platforms. *Curr. Res. Green Sust. Chem.* 4, 100127. doi:10.1016/j.crgsc.2021.100127

Xu, F. (1996). Oxidation of Phenols, Anilines, and Benzenethiols by Fungal Laccases: Correlation between Activity and Redox Potentials as Well as Halide Inhibition†. *Biochemistry* 35, 7608–7614. doi:10.1021/bi952971a

Yliperttula, M., Laurén, P., Bhattacharya, M., Lou, Y.-R., and Laukkanen, A. (2013). *Plant Derived Cell Culture Material*. United Nations, World Intellectual Property Organization.Patent WO/2012/056109.

Yu, L., Smith, J., Laskin, A., Anastasio, C., Laskin, J., and Zhang, Q. (2014). Chemical Characterization of SOA Formed from Aqueous-phase Reactions of Phenols with the Triplet Excited State of Carbonyl and Hydroxyl Radical. *Atmos. Chem. Phys.* 14, 13801–13816. doi:10.5194/acp-14-13801-2014

Zhang, Z.-Y., Sun, Y., Zheng, Y.-D., He, W., Yang, Y.-Y., Xie, Y.-J., et al. (2020). A Biocompatible Bacterial Cellulose/tannic Acid Composite with Antibacterial and Anti-biofilm Activities for Biomedical Applications. *Mater. Sci. Eng. C* 106, 110249. doi:10.1016/j.msec.2019.110249

Conflict of Interest: TL is not nor has ever been employed by VTT Technical Research Centre of Finland Ltd. She has external researcher rights to VTT and is employed by Aalto University. SA is employed by VTT, which is a non-profit research organization and the research done in this study has not been done as customer research in any part. The research has not been funded by VTT internal funding nor with customer projects but only by Academy of Finland funding. There is no conflict of interest from SA employment side.

Publisher's Note: All claims expressed in this article are solely those of the authors and do not necessarily represent those of their affiliated organizations, or those of the publisher, the editors and the reviewers. Any product that may be evaluated in this article, or claim that may be made by its manufacturer, is not guaranteed or endorsed by the publisher.